

Modified glassy carbon electrode based on myoglobin and reduced graphene oxide for hydrogen peroxide detection

A. Szöke, G. Turdean*, L. Muresan

"Babe -Bolyai" University, Faculty of Chemistry and Chemical Engineering, Department of Chemical Engineering, Research Center for Electrochemistry and Non-conventional Materials, 11 Arany Janos St., RO-400028, Cluj-Napoca, Romania

Received November 1, 2016 Revised March 6, 2016

In this work, a novel sensor (GC/Chit/rGO-Chit-Mb) for hydrogen peroxide (H_2O_2) detection was developed, based on the immobilization of myoglobin (Mb) and reduced graphene oxide (rGO) on the surface of a glassy carbon electrode in a biopolymer matrix (Chitosan, Chit). The obtained device was characterized by cyclic voltammetry (CV), amperometry and electrochemical impedance spectroscopy (EIS). The Mb modified electrode showed excellent electrocatalytic activity for the reduction of H_2O_2 in the concentration range up to 30 μM H_2O_2 with a detection limit below 10 μM H_2O_2 (by both CV and amperometry).

Key words: modified electrodes, myoglobin, reduced graphene oxide, H_2O_2 detection.

INTRODUCTION

Myoglobin (Mb) is a water-soluble single-chain protein of amino acids containing a heme (iron-containing porphyrin) group in the center, and having peroxidase-like activity, extensively used for investigating electron transfer [1]. In this regard, some problems resulted from the fact that direct electron transfer between Mb and bare solid electrode is usually very slow and the electrochemical behavior of the electrode is unstable [2, 3]. Consequently, many efforts have been made to improve the electrodes stability, as well as the electron transfer characteristics of Mb by using polymers, mediators, promoters, or other materials [4, 5].

In order to increase Mb-based electrodes stability, different matrices such as carboxymethyl cellulose (CMC) [6], polytyramine [7], Nafion [8], chitosan [9] etc. were used to immobilize Mb on pyrrolitic graphite, glassy carbon or gold. On the other hand, the electrochemical response of Mb was enhanced by introducing different conducting materials in these matrices such as gold [5] or silver nanoparticles [10], TiC nanoparticles [11], carbon nanotubes [8, 12], etc. In addition to conductivity, the nanomaterials exhibit high biocompatibility, adsorption ability and little harm to the biological activity of redox proteins.

In recent years, graphene, or its derivatives such as reduced graphene oxide (rGO) have been widely

used as modifying agents which, owing to their outstanding electronic properties and large surface area [13,14], could improve the analytical parameters of electrode materials. With its 2D sheet-like structure, graphene may act as a support for the molecular catalysts with large molecules such as Mb and other porphyrin species through cation- and π -interactions [15]. Besides, graphene derivatives have been proven to act as functional polymer reinforcements [16, 17].

Graphene-chitosan modified electrodes were successfully used for selective detection of dopamine [18, 19], nitrophenols [20], glucose [21], catechol, resorcinol and hydroquinone [22], etc. Chitosan is a conductive biopolymer derivative of chitin [23, 24] which can successfully play the role of an electrochemistry promoting polymeric binder as backbone.

In the present work, the preparation of a novel bi-layered composite electrode with large surface area, based on the glassy carbon (GC) modified by drop casting with reduced graphene oxide (rGO), myoglobin (Mb) and chitosan (Chit), GC/Chit/rGO-Chit-Mb, is reported. The intermediate Chit layer was added to improve the adhesion of the Mb containing active layer on glassy carbon and hence, the electrode stability. Detection of H_2O_2 based on direct electrochemistry of myoglobin on different electrode materials such as gold deposited on ITO [25], nanopyramidal gold surface [26], silver nanoparticles decorated oxidized multi-walled carbon nanotubes [27], glassy carbon [28,29,30], has already been reported in the literature. To the best of our knowledge, however, the electrochemical behavior of a modified electrode

To whom all correspondence should be sent:
E-mail: gturdean@chem.ubbcluj.ro

consisting from rGO, chitosan and myoglobin combination deposited on GC for H_2O_2 detection has not been the subject of a detailed investigation.

The GC/Chit/rGO-Chit-Mb electrode was characterized by cyclic voltammetry and amperometry techniques. Electrochemical impedance spectroscopy was used to get deeper insight into the modification process of the GC surface. It was found that the bi-layered composite film could provide a favorable microenvironment for Mb to realize a direct electron transfer.

EXPERIMENTAL

Reagents

The reduced graphene oxide (rGO) was provided by Chengdu Organic Chemicals Co. Ltd., Chinese Academy of Sciences. As shown in Fig. 1, the TEM image of the reduced graphene oxide sheet (rGO) presents continuous structure with dimension of nanometers.



Fig. 1. TEM micrograph of 1 mg/mL rGO dispersion in ethanol.

Myoglobin (Mb) from horse skeletal muscle ($M = 18800$ Da) was provided by Fluka. The $\text{Na}_2\text{HPO}_4 \times 2 \text{H}_2\text{O}$, $\text{NaH}_2\text{PO}_4 \times 12 \text{H}_2\text{O}$ and high viscosity chitosan from crab shells were provided by Sigma Aldrich (CAS9012-76-4). A 30% H_2O_2 solution and glacial acetic acid were provided by Merck. All chemicals were of analytical grade and used without any purification step.

A 1 mg/mL dispersion of reduced graphene oxide (rGO) was obtained by mixing the appropriate quantity of powder for 30 minutes on a vortex mixer, followed by sonication (2 hours) and mixing (30 minutes) on a vortex mixer. Before every usage, the stored dispersion was further sonicated, and then mixed for 30 minutes. A 0.1 % chitosan solution was prepared by dissolving appropriate amount of powder in 0.1 M acetic acid solution. A 10 mg/mL myoglobin solution was prepared by dissolving myoglobin in distilled water. 0.1 M phosphate buffer solutions of various pH values were prepared by dissolving appropriate amounts of Na_2HPO_4 and NaH_2PO_4 in distilled

water and adjusting the pH values with 0.1 M H_3PO_4 or NaOH solutions, respectively.

Methods

Transmission electron microscopy (TEM) measurements were performed using a H7650 Hitachi TEM apparatus.

Electrochemical measurements were performed using a PGStat 12 computer controlled potentiostat (Autolab, The Netherlands). An undivided electrochemical cell containing the modified glassy carbon electrode (GC, 3 mm diameter) as the working electrode, a platinum wire as the counter and an Ag/AgCl/KCl_{sat} as reference electrode, was connected to the potentiostat. All experiments were carried out at room temperature.

Impedance spectra were recorded in 0.5 M KCl containing 1 mM $\text{K}_3[\text{Fe}(\text{CN})_6]$ solution at the open circuit potential (OCP). Impedance spectra were analyzed by fitting to equivalent electrical circuits using the ZView (Scribner Assoc.) software.

Electrode preparation

The cleaning of glassy carbon electrodes (GC) surfaces consisted in polishing with 1200 abrasive paper and alumina powder (0.4 μm), followed by ultrasonication for 3 minutes. Between each step the electrode surface was rinsed with distilled water and the surface inspected *via* optical microscope.

The modified electrodes were prepared by drop casting technique as reported in a previous paper [19]. Thus, the GC/Chit/rGO-Chit-Mb electrodes were prepared by successive deposition of Chit (2 μL), and 10–18 μL of a mixture containing rGO dispersion (5 μL), Chit solution (5 μL) and various amounts (0, 2, 4, 6, 8 μL) of 10 mg/ml myoglobin solution. Between each deposition step, the solvent was evaporated by air drying [19]. For electrochemical impedance spectroscopy studies, GC/rGO-Chit-Mb electrodes were prepared by deposition of 12–17 μL from a mixture of Chit solution (7 μL), Mb solution (5 μL) and various amounts of rGO dispersion (0, 2.5, 5 μL) on the GC electrode surface. The solutions were deoxygenated by bubbling nitrogen prior to each experiment.

RESULTS AND DISCUSSION

3. 1. Electrochemical characterization of GC/rGO-Mb/Chit modified electrodes

The direct electron-transfer behavior of Mb at GC/Chit/rGO-Chit-Mb modified electrodes was characterized by cyclic voltammetry (CV). As seen in Fig. 2A, a pair of well-defined peaks (I_q/I_c) placed at -0.100 V and -0.350 V vs. Ag/AgCl,

KCl_{sat} , respectively, was observed on the voltammograms recorded at the modified electrode. This pair of peaks was attributed to the redox process involving the protein heme Fe(III)/Fe(II) couple, described by the following equation:



The formal potential (E^0) calculated as the arithmetic mean of the anodic and cathodic peak potentials was -0.225 V and is typical for the active center of Mb Fe(III)/Fe(II) redox couple [31]. On the other side the value of the peak potential

separation (ΔE_p) of 0.250 V confirms the quasi-reversible behavior of the redox process occurring at GC/Chit/rGO-Chit-Mb modified electrode. Having a large surface-to-volume ratio [5] and providing a suitable pathway for protein to exchange electrons with the electrode surface, the biopolymer film of chitosan and the rGO structure constitute an appropriate environment for the immobilization of Mb.

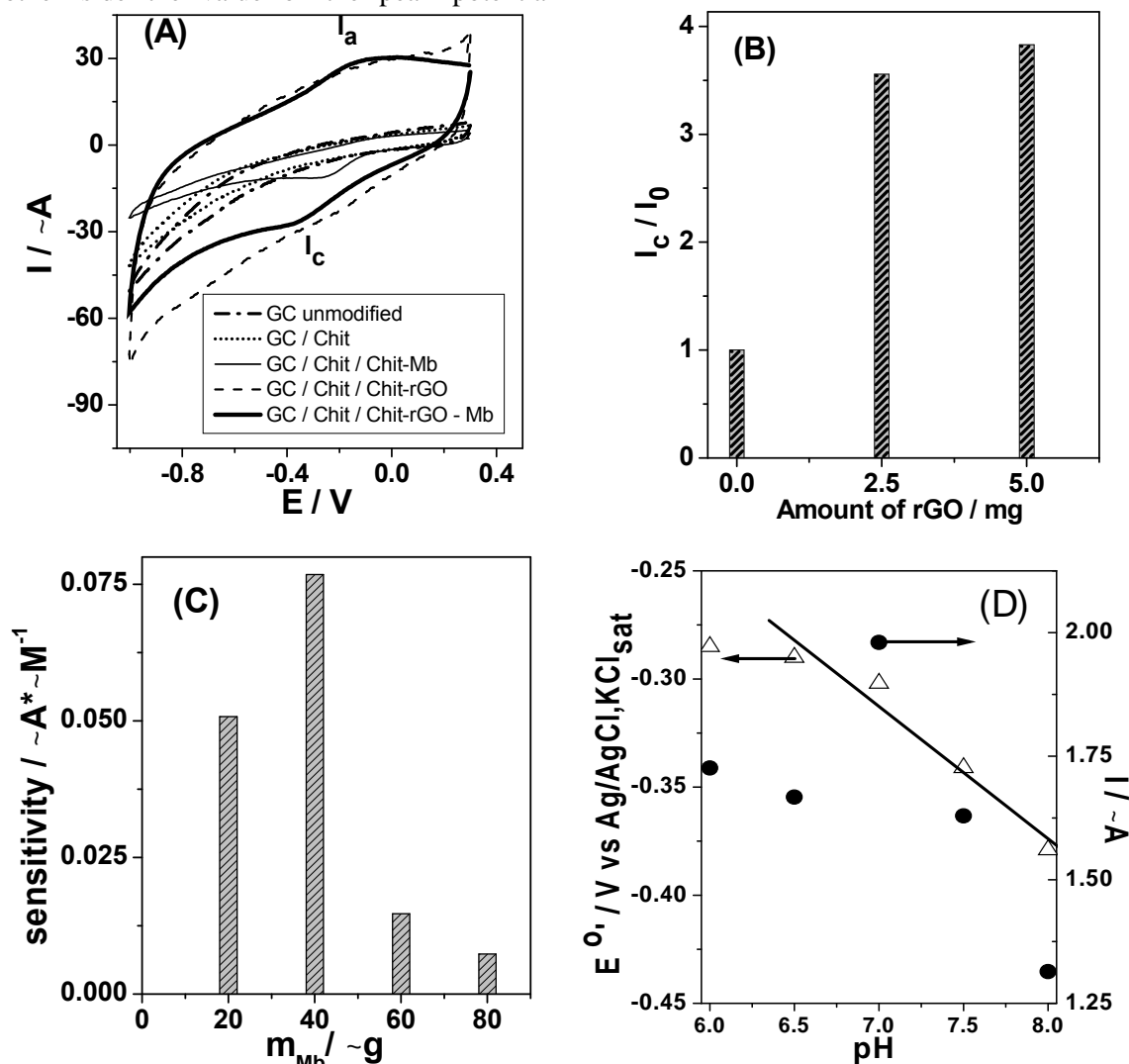


Fig. 2. Cyclic voltammograms of bare and GC/Chit/rGO-Chit-Mb modified electrodes (see legend) (A); influence of the rGO amount on the cathodic peak current intensity obtained for the detection of $10 \mu\text{M}$ H_2O_2 (B); influence of Mb amount on the sensitivity of the calibration curves of GC/Chit/rGO-Chit-Mb modified electrodes for H_2O_2 detection (C); influence of the pH on the cathodic peak current and the formal potential (D). Experimental conditions: electrolyte, 0.1 M phosphate buffer (pH 7); starting potential $+0.3$ V vs. $\text{Ag}/\text{AgCl}, \text{KCl}_{\text{sat}}$; scan rate, 0.050 V s^{-1} .

For an immobilized redox species, the surface coverage can be estimated from the slope of the Laviron equation: $I_p = n^2 F^2 A X \epsilon / (4RT)$, where I_p is the peak current value in A, n is the number of electron transferred in the electrode reaction, F is Faraday constant, A is the effective surface area of

the modified electrode in cm^2 , X is the surface coverage of the immobilized Mb in mol/cm^2 , ϵ is the scan rate in V/s , R is the universal gas constant in $\text{J}/(\text{mol K})$, and T is the absolute temperature (298.15 K) [32, 33]. Thus, for the GC/Chit/rGO-Chit-Mb modified electrode in the scan rate range

from 0.01–0.1 V s⁻¹, the average X value was calculated as 1.89 10⁻¹⁰ mol/cm². As expected for the present electrode architecture, the value of X is much larger than the reported for a monolayer coverage (1.58 10⁻¹¹ mol/cm² [34] or 1.89 10⁻¹¹ mol/cm² [35]). Ten times higher value of X suggests that: (i) a multilayer of Mb participated to the electron transfer pathway within the electrode matrix [36], or (ii) the rGO-Chitosan matrix provides a high surface area for Mb immobilization [37], allowing a proper orientation and homogenous distribution of the Mb active sites on the electrode surface [38].

Influence of rGO amount

Although the position of the peak potential for the GC/Chit/rGO-Chit-Mb electrode remains almost the same regardless the amount of rGO used for the preparation of the electrode material, the current intensity ratio has changed. As shown in Fig. 2B, the ratio of the cathodic peaks I_c/I₀ (where I₀ is the current peak in the absence of rGO from the electrode matrix) shows an increase of 3.5–4 times in the presence of rGO, reaching a quasi-stable value at 2.5–5 µg of rGO. Consequently, a value of 5 µg of rGO was considered sufficient and appropriate for modifying the electrode surface.

Influence of Mb amount

The influence of the Mb amount on the analytical performances of the modified electrodes was expressed by means of the electrode sensitivity, calculated as the slope of the linear domain of the calibration curve for H₂O₂ detection obtained by cyclic voltammetry. As seen in Fig. 2C, the electrode sensitivity shows a polynomial dependence on the amount of Mb immobilized on the electrode surface having a maximum value for 40 µg Mb.

pH influence

The redox behavior of Mb is significantly dependent on the pH of solution, because the microstructure of protein undergoes conformational changes. Therefore, the influence of the pH of 0.1 M phosphate buffer solution on the cyclic

voltammetric behavior of GC/Chit/rGO-Chit-Mb modified electrode was investigated in the pH range from 6.0 to 8.0. As shown in Fig 2D, the linear dependence of the formal potential (E^{0'}) of the immobilized Mb has a negative slope with the increase of the electrolyte pH. The slope value obtained from the linear fitted equation, E^{0'}/V = -(0.061 ± 0.009)pH + (0.116 ± 0.066) (n = 4, R= 0.9785), is found to be close to the theoretical value of 0.059 V/pH at 25^o C for a reversible 1e⁻ transfer. Also, this slope value could indicate that each electron transfer from the Mb to the electrode is accompanied by 1 H⁺, according to the modified equation (1a):



This behavior has usually been explained in the literature either by the influence of protonation states of the trans-ligands to the Heme iron and the amino acids around the Heme, or by protonation of the water molecule coordinated to the central iron [4]. As shown in Fig. 2D, the cathodic peak current intensities have a non-linear dependency on the pH with a maximum value observed at pH 7.0 that was selected as the working pH in further investigations.

Influence of the scan rate

The influence of the potential scan rate (v) on the voltammetric responses of GC/Chit/rGO-Chit-Mb modified electrode is presented in Fig. 3, where the pair of well-defined redox peaks with almost equal anodic/cathodic peak current intensities can be observed. The redox peak currents increased linearly with the scan rates from 0.01 to 0.25 V s⁻¹ (results not shown). The values of the slopes, calculated by linear regression of the log I - log v dependencies, were found to be 0.678 and 0.715, respectively (Table 1), indicating a typical thin-layer surface-controlled electrochemical response of the Mb immobilized on the electrode surface [5,40]. Increase of the potential scan rate leads to the shifting of the voltammograms and to a gradual enlargement of the peak-to-peak separation (E_p), confirming the existence of a quasi-reversible electrode process.

Table 1. Parameters of the log-log linear regression corresponding to the peak current - potential scan rate dependence at the GCE/Chit/rGO-Chit-Mb modified electrode. Experimental conditions as in Fig. 3.

Electrode	Slope of the log I _p – log v dependence			
	reduction	R ² /n	oxidation	R ² /n
GCE/Chit/Mb/Chit/rGO	0.715 ± 0.065	0.9602/11	0.678 ± 0.032	0.9891/11

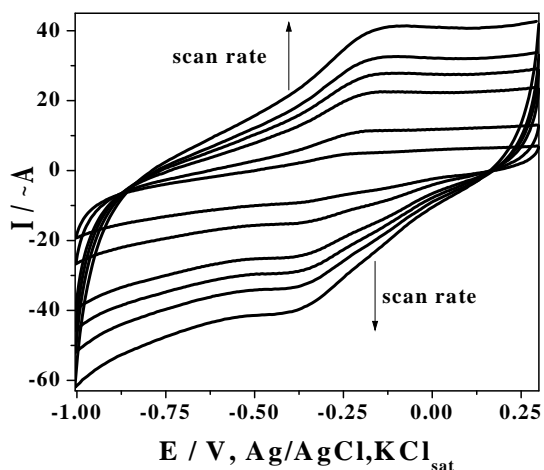


Fig. 3. Influence of the scan rate (0.010 – 0.080 V s⁻¹) on cyclic voltammograms of the GC/Chit/rGO-Chit-Mb modified electrode. Experimental conditions: electrolyte, 0.1 M phosphate buffer (pH 7); starting potential +0.3 V vs. Ag/AgCl, KCl_{sat}.

Short time stability

The short time stability of the electrochemical response of the GC/Chit/rGO-Chit-Mb modified electrode was very good. The continuous scanning in a potential window of 1.3 V (from +0.3 V to -1 V) did not affect significantly the cyclic voltammetric signals. As shown in Fig. 4, the time dependencies of anodic and cathodic peak currents follow the first order kinetic in either absence or presence of H₂O₂, proving a good stability of the modified electrode (deactivation constants are between 3.05 × 10⁻¹¹ and 4.5 × 10⁻¹¹ s⁻¹).

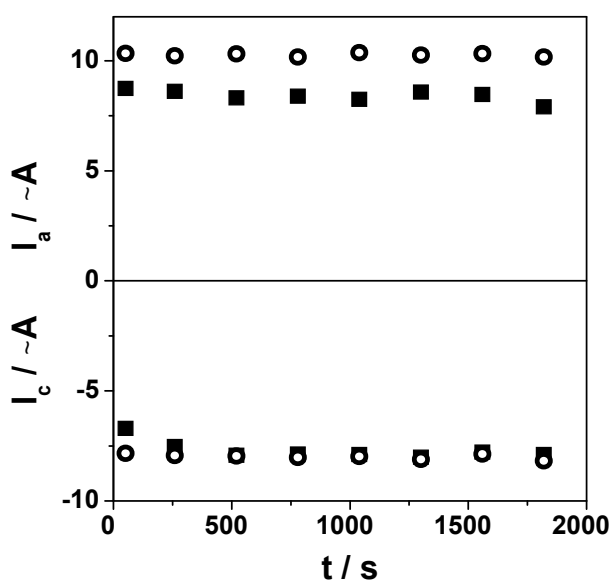


Fig. 4. I_c and I_a versus time dependencies of the GC/Chit/rGO-Chit-Mb modified electrode recorded by CV before (■) and after addition of 40 μM H₂O₂ (○). Experimental conditions: electrolyte, 0.1 M phosphate buffer (pH 7); starting potential +0.3 V vs. Ag/AgCl, KCl_{sat}; scan rate, 0.050 V s⁻¹.

EIS measurements

In order to better understand the role of every component of the modifier layer and to get more information regarding the modified GC surface, electrochemical impedance spectroscopy (EIS) was applied. Impedance spectra of GC, GC/Chit-Mb and GC/rGO-Chit-Mb electrodes, measured at the open-circuit potential in 0.5 M KCl containing 1mM K₃[Fe(CN)₆] solution, are presented as Nyquist plots (Z'' vs. Z') in Fig. 5.

Usually, the Nyquist representations of EIS spectra for redox reactions include a semicircle portion at higher frequencies, corresponding to the electron transfer limited process and a linear portion at lower frequencies, corresponding to the diffusion process. The diameter of the semicircle part recorded at higher frequencies is equal to the electron transfer resistance (R_{ct}) at the electrode interface, which controls the electron transfer kinetics of the redox probe at the electrode interface [39].

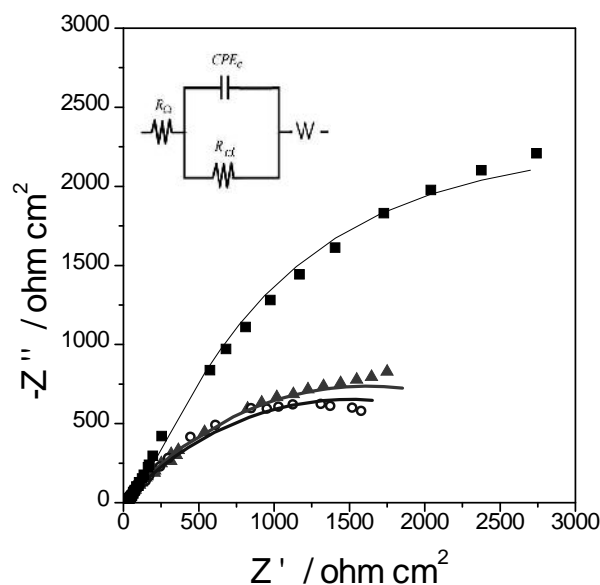


Fig. 5. Nyquist plots for different types of modified electrodes: GCE (■), GCE/Chit-Mb (●), GCE/rGO-Chit-Mb (○) at open-circuit potential value. Experimental conditions: electrolyte, 1 mM K₃[Fe(CN)₆] solution containing 0.5 M KCl; frequency range, 10⁻² - 10⁵ Hz; perturbation amplitude, 5 mV. Inset: schemes of the equivalent circuits used for fitting the experimental data.

In our case, two equivalent circuits, R(QR_{ct}) and R(CR_{ct})W (insets in Fig. 5), including electrolyte resistance (R), constant phase element for double-layer capacitance (Q), active charge transfer resistance (R_{ct}), and Warburg impedance (W) were used to fit impedance data of GC/Chit-Mb and GC/rGO-Chit-Mb electrodes and GC electrode, respectively.

Using the above-mentioned equivalent circuits, the values of R_{ct} for the bare GC, GC/Chit-Mb and GC/rGO-Chit-Mb modified electrodes were estimated. The lowest value was noticed for the GC and higher for the two modified electrodes, suggesting that as expected, the chitosan layer hinders the charge transfer of the redox probe $[\text{Fe}(\text{CN})_6]^{3-/4-}$ at the electrode surface. The capacitance values increased somewhat by addition of rGO (GC/Chit-Mb ($316.2 \mu\text{F}/\text{cm}^2$) < GC/Chit/Chit-rGO-Mb ($386.8 \mu\text{F}/\text{cm}^2$)), which is probably due to an increase in the electroactive area of the electrode. The complex architecture of the electrode matrix, containing chitosan and 2D porous structure of rGO provide the expected largely exposed surface area with high activity, which permits the electron transfer from the redox probe $[\text{Fe}(\text{CN})_6]^{3-/4-}$ to reach the electrode surface [5,39,40]. As expected, the impedance spectra demonstrate that both resistivity and electrode surface structure changed with the modification of the GC surface.

3.2. Electrocatalytic effect

The electrocatalytic activity of GC/Chit/rGO-Chit-Mb modified electrode towards H_2O_2 was studied by cyclic voltammetry and illustrated in Fig. 6A. When increasing concentrations of H_2O_2 were added to the buffer solution, the following typical phenomena, characteristic for electrocatalysis, were observed: (i) shifting and in this case splitting of the Mb peak into two peaks (I_c , II_c) placed at -0.340 V and -0.15 V vs. Ag/AgCl , KCl_{sat} respectively and (ii) increase of the II_c peak current intensity accompanied by simultaneous decrease of the oxidation peak (I_a).

Two reduction peaks are attributed to the peroxidase-like electrocatalytic reactions which can be involved in the reduction of Mb Heme Fe(III) to Heme Mb Fe(II), and the reduction of H_2O_2 at the Mb modified electrode, according to the following equations [41,42]:

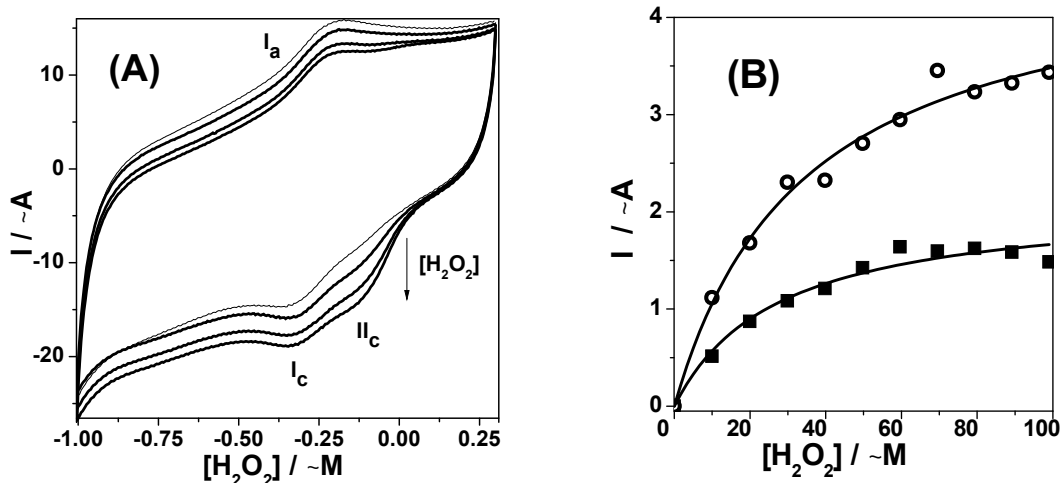
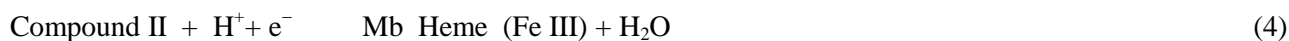
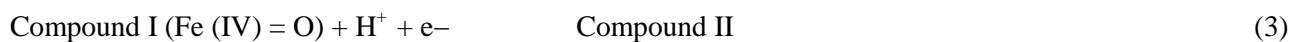
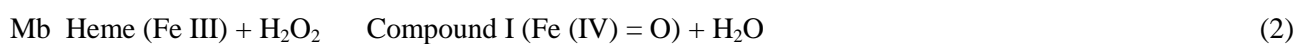


Fig. 6. Cyclic voltammograms of GC/Chit/rGO-Chit-Mb modified electrodes before (thin black line) and after addition of various (30, 40, 50 μM) H_2O_2 concentrations (thick black lines) (A); calibration curves for H_2O_2 electroreduction at GC/Chit/Chit-Mb (■) and GC/Chit/rGO-Chit-Mb (●) modified electrodes (B). Experimental conditions: electrolyte 0.1 M phosphate buffer (pH 7); starting potential $+0.3 \text{ V}$ vs. Ag/AgCl , KCl_{sat} ; scan rate 0.050 V s^{-1} .

Table 2. Analytical parameters of the calibration curves for H_2O_2 electroreduction at the GCE/Chit/rGO-Chit-Mb modified electrode.

Amount of rGO [μg]	Sensitivity [$\mu\text{A} / \mu\text{M}$]	Limit of detection [μM]	Linear domain [μM]	R/n
0	0.076 ± 0.009	8.83	10....30	0.9830 / 4
5	0.152 ± 0.016	7.91		0.9863 / 4



A good linear relationship between the current intensity of the reduction peak II_c and H_2O_2 concentration was obtained in the range 10–30 μM , with a sensitivity between 0.076 and 0.152 $\mu A/\mu M$ in the absence and presence of rGO in the modifying matrix of the electrode, respectively (Fig. 6B, Table 2). The detection limit calculated for a signal/noise ratio of 3 was in both cases below 10 $\mu M H_2O_2$.

When the H_2O_2 concentration was up to 30 μM , the current intensity of peak II_c leveled off, reaching a saturation value and indicating a Michaelis-Menten kinetic for the electrocatalytic reaction of H_2O_2 . The apparent Michaelis-Menten constant ($K_{M,app}$) calculated using Origin 6.5 software fitting facility, was equal to 27.2 μM for GC/Chit/Chit-Mb and to 34.2 μM for GC/Chit/rGO-Chit-Mb electrodes, respectively. The obtained values for $K_{M,app}$ are smaller or similar to those reported in the literature [5,36,39], proving that the Mb shows affinity for the studied substrate (H_2O_2).

In order to quantitatively investigate the catalytic properties of GC/Chit/rGO-Chit-Mb modified electrodes, I vs. time dependencies were recorded by amperometry at applied potential of -0.3 V vs. Ag/AgCl, KCl_{sat} for successive additions of 5 $\mu M H_2O_2$ solution. The reduction current reaches a stable 95% of steady-state value within 100 s after each addition of H_2O_2 , suggesting that sufficiently fast electrocatalytic response was achieved. The analytical parameters of the GC/Chit/rGO-Chit-Mb modified electrode extracted from the amperometric linear calibration curve presented in Fig. 7 were: sensitivity of $0.047 \pm 0.003 \mu A/\mu M$, linear range of 5–30 μM and detection limit of 4.99 $\mu M H_2O_2$ ($R = 0.9929$).

Thus, the detection limit recorded at GC/Chit/rGO-Chit-Mb modified electrode is in agreement with other values reported for similar electrode architectures for signal/noise ratio = 3 (i.e.: 1.02 $\mu M H_2O_2$ at Chit-MWNTs/Mb/AgNPs/GCE [36]; 1.5 μM at Mb/SGO/Nafion electrode [39]; 6 $\mu M H_2O_2$ at Nafion/Mb/MWCNTs/CILE [40]; 40 $\mu M H_2O_2$ at Mb-DTAB/Ceramic carbon electrode [32]). Even if the analytical parameters of the GC/Chit/rGO-Chit-Mb modified electrode are not high enough, the periodical scanning of the potential did not affect the electrochemical signal (see Fig 4), so that the compromise between the analytical parameters values and the stability of the electrochemical response of the GC/Chit/rGO-Chit-Mb modified electrode can be considered acceptable.

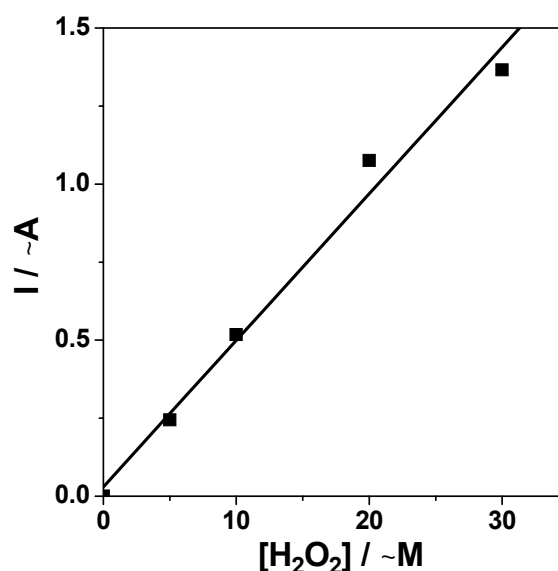


Fig. 7. Linear domain of the amperometric calibration curve for H_2O_2 electroreduction at GCE/rGO-Chit-Mb modified electrodes. Experimental conditions: electrolyte, 0.1 M phosphate buffer (pH 7); potential -0.3 V vs. Ag/AgCl, KCl_{sat} ; rotation speed, 250 rpm.

CONCLUSIONS

Chitosan and rGO can act as an effective support matrix for Mb immobilization in view to prepare a novel GC/Chit/rGO-Chit-Mb modified electrode by drop-casting method. Direct electrochemistry of the immobilized Mb on the modified electrode was carefully investigated by cyclic voltammetry, amperometry and electrochemical impedance spectroscopy. The experimental results showed that the immobilized Mb displayed good enzyme-like catalytic activity for the reduction of H_2O_2 , characterized by good analytical and kinetic parameters.

These results suggest that the modified matrix of the studied electrodes appears to be a promising material for fabricating electrochemical sensors based on the direct electrochemistry of a redox protein.

Acknowledgements. The authors thank Dr. Katona Gabriel for the TEM measurements.

REFERENCES

1. C. U. Carlsen, I. M. Skovgaard, L. H. Skibsted, *J. Agric. Food Chem.*, **51**, 5815 (2003).
2. H. Huang, N. F. Hu, Y. H. Zeng, G. Zhou, *Anal. Biochem.*, **308**, 141 (2002).
3. K. Chattopadhyay, S. Mazumdar, *Bioelectrochem.*, **53**, 17 (2000).
4. C. Ruan, T. Li, Q. Niu, M. Lu, J. Lou, W. Gao, W. Sun, *Electrochim. Acta*, **64**, 183 (2012).
5. F. Shi, J. Xi, F. Hou, L. Han, G. Li, S. Gong, C. Chen, W. Sun, *Mater. Sci. Eng. C*, **58**, 450 (2016).

6. H. Huang, P. He, N. Hu, Y. Zeng, *Bioelectrochem.*, **61**, 29 (2003).
7. A. T. Ezhil Vilian, V. Veeramani, S.-M. Chen, R. Madhu, C. H. Kwak, Y. S. Huh, Y.-K. Han, *Sci. Rep.*, **5**, 18390 (2015), doi:10.1038/srep18390.
8. E. Canbay, B. ahin, M. Kiran, E. Akyilmaz, *Bioelectrochem.*, **101**, 126, (2015).
9. L.-S. Duan, Q. Xu, F. Xie, S.-F. Wang, *Int. J. Electrochem. Sci.*, **3**, 118 (2008).
10. S. Palanisamy, C. Karuppiyah, S.-M. Chen, R. Emmanuel, P. Muthukrishnan, P. Prakash, *Sens. Actuat. B*, **202**, 177 (2014).
11. M. Wang, Q. Sheng, D. Zhang, Y. He, J. Zheng, *Bioelectrochem.*, **86**, 46 (2012).
12. G. L. Turdean, G. Szabo, *Food Chem.*, **179**, 325 (2015).
13. V. B. Mohan, R. Brown, K. Jayaraman, D. Bhattacharyya, *Mater. Sci. Eng. B*, **193**, 49 (2015).
14. M. Cui, B. Xu, C. G. Hu, H. B. Shao, L. Y. Qu, *Electrochim. Acta*, **98**, 48 (2013).
15. T. Xue, S. Jiang, Y. Qu, Q. Q. Su, R. Cheng, S. Dubin, Ch-Y. Chiu, R. Kaner, Y. Huang, X. Duan, *Angewandte Chem. Int. Ed.*, **51**, 3822 (2012).
16. G. Mittal, V. Dhand, K. Y. Rhee, S.-J. Park, W. R. Lee, *J. Ind. Eng. Chem.*, **21**, 11 (2015).
17. K. Hu, D. D. Kulkarni, I. Choi, V. V. Tsukruk, *Prog. Poly. Sci.*, **39**, 1934 (2014).
18. Y. Wang, Y. Li, L. Tang, J. Lu, J. Li, *Electrochem. Commun.*, **11**, 889 (2009).
19. Á. F. Szöke, G. L. Turdean, G. Katona, L. M. Muresan, *Stud. UBB Chem.*, **61(3)**, 135 (2016).
20. J. Tang, L. Zhang, G. Han, Y. Liu, W. Tang, *J. Electrochem. Soc.*, **162(10)**, B269 (2015).
21. X. Kang, J. Wang, H. Wu, I. A. Aksay, J. Liu, Y. Lin, *Biosens. Bioelectron.*, **25(4)**, 901 (2009).
22. H. Yin, Q. Zhang, Y. Zhou, Q. Ma, T. Liu, L. Zhu, S. Ai, *Electrochim. Acta*, **56**, 2748 (2011).
23. J. B. Marroquin, K.Y. Rhee, S.J. Park, *Carbohydrate Polymers*, **92 (2)**, 1783 (2013).
24. M. Rinaudo, *Prog. Poly. Sci.*, **31(7)**, 603 (2006).
25. Dengale S. M., Yagati A. K., Chung Y. H., Min J., Choi J. W., *J. Nanosci. Nanotechnol.*, **13**, 6424 (2013).
26. P. Xia, H. Liu, Y. Tian, *Biosens. Bioelectron.*, **24**, 2470 (2009).
27. B. Liu, M. Wang, *J. Electrochem. Sci.*, **8**, 9801 (2013).
28. A. Safavi, F. Farjami, *Anal. Biochem.*, **402**, 20 (2010).
29. L.-S. Duan, Q. Xu, F. Xie, S.-F. Wang, *Int. J. Electrochem. Sci.*, **3**, 118 (2008).
30. A. Babaei, A. R. Taheri, *Anal. Bioanal. Electrochem.*, **4**, 342, (2012).
31. Y. Z. Zhou, H. Wang, S. Y. Dong, A. X. Tian, Z. X. He, B. Chen, *Chin. Chem. Lett.*, **22**, 465 (2011).
32. E. Laviron, *J. Electroanal. Chem.*, **101**, 19 (1979).
33. A. J. Bard, L. R. Faulkner, *Electrochemical Methods: Fundamentals and applications*, Wiley, New York, 2001.
34. S. F. Wang, T. Chen, Z. L. Zhang, X. C. Shen, Z. X. Lu, D. W. Pang, K. Y. Wong, *Langmuir*, **21(20)**, 9260 (2005).
35. S. F. Wang, T. Chen, Z. L. Zhang, D. W. Pang, K. Y. Wong, *Electrochem. Commun.*, **9**, 1709 (2007).
36. Y. Li, Y. Li, Y. Yang, *Bioelectrochem.*, **82**, 112 (2011).
37. S. Pakapongpan, R. Palangsuntikul, W. Surareungchai, *Electrochim. Acta*, **56**, 6831 (2011).
38. S. Ray, S. Chand, Y. Zhang, S. Nussbaum, K. Rajeshwar, R. Perera, *Electrochim. Acta*, **99**, 85 (2013).
39. G. Chen, H. Sun, S. Hou, *Anal. Biochem.*, **502**, 43 (2016).
40. W. Sun, X. Li, Y. Wang, X. Li, C. Zhao, K. Jiao, *Bioelectrochem.*, **75**, 170 (2009).
41. Y. Zhang, Z. Xia, H. Liu, M. Yang, L. Lin, Q. Li, *Sens. Actuat. B*, **188**, 496 (2013).
42. G. L. Turdean, *Studia UBB Chem.*, **60(3)**, 119 (2015).

-

*, .

“

’ .A 11, RO-400028,

1 2016 .; 6 2017 .

()

(GC / Chit / RGO-Chit-Mb) (2 2)

(Mb) (RGO)

(Chitosan, Chit).

(CV),

(EIS). (Mb)

2 2 2 2 30 μM 10μM 2 2 (CV

).